

# CDCNET: A FAST AND LIGHTWEIGHT DEHAZING NETWORK WITH COLOR DISTORTION CORRECTION

*Yilian Zhong<sup>1</sup>, Jiaming Liu<sup>1</sup>, Xuan Huang<sup>1</sup>, Jingjing Liu<sup>2</sup>, Yibo Fan<sup>1</sup>, Minfeng Wu<sup>3\*</sup>*

<sup>1</sup> School of Microelectronics, Fudan University

<sup>2</sup> School of Microelectronics, Shanghai University

<sup>3</sup> Huadong Hospital Affiliated to Fudan University, Shanghai, 200040, China

## ABSTRACT

Mobile edge devices require real-time dehazing methods that sustain dehazing performance while drastically reducing resource occupation. However, color distortion is a substantial challenge for lightweight dehazing networks, which profoundly impairs image quality. In this paper, we propose CDCNet, a fast and lightweight dehazing network with color distortion correction, to tackle these challenges. Firstly, CDCNet utilizes a multi-scale feature aggregation module to retain lightweight and leverages a parallel attention module to expedite the dehazing process. Secondly, we devise proportional residual connection and loss functions to mitigate potential color distortion in CDCNet. Thirdly, we design a post-processing module to adjust HSV and Lab color spaces to eliminate color distortions comprehensively. Experiments demonstrate that CDCNet surpasses state-of-the-art lightweight dehazing methods and exhibits superiority in execution time.

**Index Terms**— Image Dehazing, Lightweight, Multi-scale Feature, Attention Model, Color Distortion Correction

## 1. INTRODUCTION

Haze often deteriorates outdoor images by causing information loss and distorting colors, which affects object detection [1] and autonomous vehicles [2]. Therefore, image dehazing methods are extensively applied, and mobile edge devices have high requirements for memory and real-time performance. Consequently, restoring clear and color-authentic images from hazy counterparts has become a formidable challenge in real-time processing with the lightweight dehazing method. Traditional dehazing methods [3, 4] exhibit limited abilities under complex hazy conditions.

Deep learning methods demonstrate remarkable capabilities in dehazing tasks. However, the complexity of these models presents challenges for the device with limited resources, thereby inducing significant latency. Numerous researches [5, 6] focus on rectifying pixel-level information in images but frequently neglect the pivotal role of color in visual perception. In lightweight dehazing networks [7, 8, 9], color

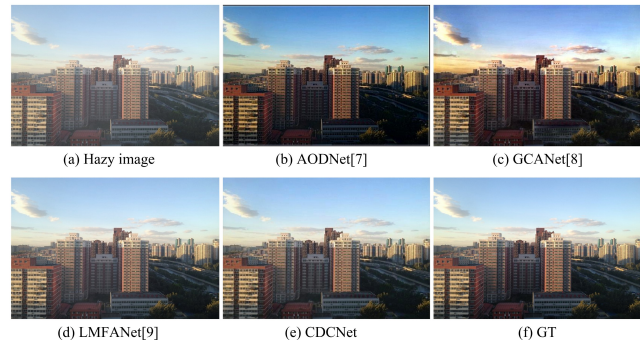


**Fig. 1.** Comparison of CDCNet with other lightweight dehazing networks on the outdoor image.

distortion is even more prominent. Due to the streamlining of models and reduction of parameters, lightweight dehazing networks cannot restore the color of hazy images accurately, intensifying the divergence from the ground truth and diminishing the perceptual quality. Figure 1 shows that the dehazed results of AODNet [7] and GCANet [8] are too dark and contain color distortions; LMFANet [9]'s result has haze residual; our CDCNet's result is clear and realistically natural.

Our contribution can be summarized as follows:

- 1) We propose a novel end-to-end fast and lightweight dehazing network with color distortion correction (CDCNet). The multi-scale feature aggregation module streamlines the network and amplifies the dehazing performance. The parallel attention module expedites the dehazing process. Furthermore, we design loss functions to mitigate the potential color distortions.
- 2) We formulate a color distortion correction module to solve the problem comprehensively. The model involves a dual-optimization strategy in HSV and Lab color space. This strategy includes a specialized non-linear stretching algorithm and meticulous luminance adjustment to eliminate color distortions.
- 3) Experiments indicate that our proposed CDCNet surpasses state-of-the-art lightweight dehazing methods quantitatively and qualitatively. Furthermore, CDCNet boasts significant advantages in execution time, enabling real-time dehazing.

\*Corresponding author: drwuminfeng1002@163.com.

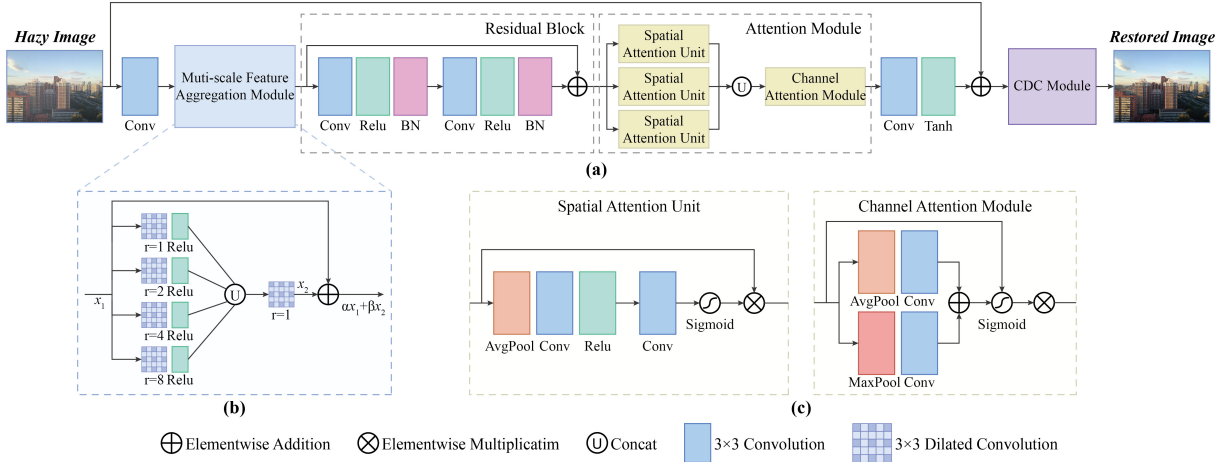


**Fig. 2.** The architecture of the proposed CDCNet. It consists of a fast and lightweight dehazing network and a color distortion correction module (CDC Module). The network has light parameters with a multi-scale feature aggregation module and attention module. Residual block facilitates information flow and enhances feature learning. We employ the CDC module to rectify the color distortion of the image, producing clear and natural results.

## 2. PROPOSED METHOD

### 2.1. A Fast and Lightweight Dehazing Network

We propose a fast and lightweight dehazing network to minimize color distortions. Figure 2(a) shows that our network strategically predicts the global residual between hazy images and their clear counterparts. This strategy augments our network's efficacy capacity to restore the images' tonal quality and details. The prediction of the network can be described as follows:

$$R(x) = J(x) - I(x), \quad (1)$$

where  $R(x)$  represents the global residual,  $I(x)$  is the hazy image, and  $J(x)$  is the corresponding clear image.

**Multi-scale Feature Aggregation Module.** Utilizing multi-scale features has been proven to enhance the image dehazing performance of networks [10, 11, 12]. We design a multi-scale feature aggregation module with limited channels to maintain our network compactness. Figure 1(b) shows that the 12-channel input feature  $x_1$  directs to four sets of dilated convolution layers operating in parallel, effectively leveraging features from various scales. Although each convolution kernel measures  $3 \times 3$  in size, the dilation rates are 1, 2, 4, 8, and ensure that larger dilation rates encompass a wide receptive field for the global characteristics. In comparison, lower rates target intricate local details. After ReLU activation, features are combined and fused by a standard  $3 \times 3$  2D convolution. The output feature  $x_2$  is formulated as:

$$x_2 = conv(\bigcup_{r=1,2,4,8} relu(conv(x_1))), \quad (2)$$

where  $conv$  represents the  $3 \times 3$  dilation convolution,  $\cup$  is the concat, and  $r$  is the dilation rate.

To mitigate the over-adjustment of features, we apply a proportional residual connection [13, 14] to combine the original feature and module output. This strategy ensures that our network retains the original color information while extracting pivotal features and countering color distortions. The proportional residual connection can be expressed as :

$$y = \alpha x_1 + \beta x_2, \quad (3)$$

where  $y$  represents the final output feature and the scaling parameter satisfies  $\alpha + \beta = 1$ .

**Attention Module.** Figure 1(c) shows that we integrate spatial and channel attention models [15] to make the network more lightweight. The attention mechanism reduces redundancy through adaptive weights and enhances our network's generalization.

We architect parallel multi-scale spatial attention modules to capture intricate features from hazy images and dramatically accelerate dehazing speeds. Subsequently, outputs from these spatial attention units are consolidated into the channel attention module, emphasizing channels inherently associated with haze. We combine global average pooling with maximum pooling, producing a precise channel attention map.

### 2.2. Loss Function

$L_1$  Loss calculates the absolute pixel difference between the CDCNet dehazed result and the clear image, aiding CDCNet in learning global residuals.

Lab Loss transforms the CDCNet dehazed result and clear image from RGB to Lab color space [16] and computes the squared pixel difference, similar to  $L_2$  Loss, ensuring authentic colors in the dehazed result. The RGB to Lab conversion



**Fig. 3.** Visual results of CDCNet and other methods on the SOTS dataset. The results by other methods contain some color distortions and haze residual, while the dehazed image by our method is much clearer with more details.

process is detailed as follows:

$$\begin{bmatrix} X \\ Y \\ Z \end{bmatrix} = \begin{bmatrix} 0.4124 & 0.3576 & 0.1805 \\ 0.2126 & 0.7152 & 0.0722 \\ 0.0193 & 0.1192 & 0.9505 \end{bmatrix} \begin{bmatrix} \gamma^{-1}(R) \\ \gamma^{-1}(G) \\ \gamma^{-1}(B) \end{bmatrix}, \quad (4)$$

$$L = g(Y), a = h(X, Y), b = i(Y, Z), \quad (5)$$

where  $\gamma^{-1}(x)$  represents the lifting gamma gain,  $g(x)$ ,  $h(x)$ , and  $i(x)$  represent the respective nonlinear transformations from XYZ to Lab color space.

Contrastive Loss measures the perceptual difference between positive and negative samples from the pre-trained VGG16 model's various layers [17]. This contrastive regularization makes the image colors more closely to visual perception. The Contrastive Loss can be described as:

$$L_C = \sum_{i=1}^n \omega_i \cdot \frac{\|\phi_i(\hat{J}) - \phi_i(J)\|}{\|\phi_i(\hat{J}) - \phi_i(I)\|}, \quad (6)$$

where  $\omega_i$  represents the weight coefficient, and  $\phi_i$  is the output from the corresponding VGG16 layer.

To train our network for less color distortions, we weigh all the mentioned loss functions into a composite loss function, which can be expressed as:

$$L = \lambda_1 L_1 + \lambda_2 L_2 + \lambda_C L_C, \quad (7)$$

where  $\lambda_1$ ,  $\lambda_2$ , and  $\lambda_C$  are weight parameters selected based on network optimization experiments.

### 2.3. Color Distortion Correction Module

While our dehazing network significantly mitigates such color distortions, avenues for refinement and enhancement still exist. To comprehensively solve this problem, we introduce a color distortion correction module (CDC Module) into our network as a post-processing step. This module compensates for the loss of color in dehazed images. Initially, we convert the image from RGB to HSV color space. Haze often causes saturation decrease, resulting in faded colors. By non-linearly stretching the saturation in HSV color space, we selectively augment color intensity, making the image more consistent with real-world scenes. This process can be represented as:

$$\tau(S, p) = \begin{cases} 0.5 + 0.5 \left( \frac{S - 0.5}{0.5} \right)^2 & 0.5 < S \leq 1, \\ 0.5 \left( 1 - \left( 1 - \frac{S}{0.5} \right)^p \right) & S \leq 0.5, \end{cases} \quad (8)$$

where  $\tau(S, p)$  is the adaptive stretch function for  $S$ ,  $S$  represents the saturation component,  $p$  is the power constant.

Subsequently, we convert the image from HSV to Lab color space. The Lab color space closely resembles human visual perception. Hazy images experience a degradation of color and an interference in their luminance. By fine-tuning the  $L$  component in Lab color space, we optimize areas affected by residual haze or overexposure, making the image more natural. This adjustment can be represented as:

$$\eta(L, \gamma) = \gamma L, \quad (9)$$

where  $\eta(L, \gamma)$  is the finely tuned function for  $L$ ,  $L$  represents the luminance component, and  $\gamma$  is the weight parameter for the luminance adjustment.

Finally, we convert the color-corrected image from Lab to RGB color space.

## 3. EXPERIMENTS

### 3.1. Experiments Settings

Because the outdoor hazy images are more realistic in practical applications, we only focus on the evaluation of outdoor hazy images. The experiment uses the Outdoor Training Set (OTS) from the live dataset [18] for training, with a learning rate of 0.0001, batch size of 24, and the Adam optimizer. The network is trained for 50 epochs, halving the learning rate every 10 epochs. CDCNet's performance is assessed using the Synthetic Objective Testing Set (SOTS), its dehazing generalization capabilities with the Hybrid Subjective Testing Set (HSTS), and its efficacy in eliminating color distortions with the HAZERD dataset [19]. The CDC Module is active only during inference.

**Table 1.** Quantitative comparisons with SOTA methods on the synthetic and real-world dehazing datasets.

Type	Method	SOTS-outdoor		HAZERD
		PSNR↑	SSIM↑	CIEDE2000↓
Traditional	DCP[3]	19.13	0.8148	17.901
	CAP[4]	18.10	0.7562	-
Intricate	DCDPN[5]	17.48	0.8317	14.624
	FFANet[6]	33.57	0.9840	12.237
Lightweight	MSCNN[20]	19.47	0.8372	14.806
	DehazeNet[10]	22.46	0.8541	-
	AODNet[7]	20.29	0.8765	16.674
	GCANet[8]	20.56	0.7634	11.720
	LMFANet[9]	24.76	0.9336	-
	<b>CDCNet</b>	<b>26.05</b>	<b>0.9518</b>	<b>11.559</b>



**Fig. 4.** Visual results of CDCNet and other methods on the real-world image. The proposed method generates clearer dehazed images with less color distortions.

**Table 2.** Quantitative comparisons with SOTA methods of the platform, parameters, model size, and execution time

Method	Platform	Parameter(M)	Model size(KB)	Execution times(S)
DCP[3]	Matlab	-	-	1.627
CAP[4]	Matlab	-	-	0.958
DCDPN[5]	Pytorch	66.89	261734	0.849
FFANet[6]	Pytorch	4.68	21811	0.566
MSCNN[20]	Matlab	0.0084	33.55	1.740
DehazeNet[10]	Matlab	0.0083	31.20	1.402
AODNet[7]	Pytorch	<b>0.00018</b>	<b>8.71</b>	0.036
GCANet[8]	Pytorch	0.70	2755	0.109
LMFANet[9]	Pytorch	0.120	53.70	0.120
<b>CDCNet</b>	Pytorch	<b>0.101</b>	<b>39.20</b>	<b>0.017</b>

### 3.2. Results

The CDCNet is compared both qualitatively and quantitatively with other state-of-the-art (SOTA) methods. Table 1 reveals that CDCNet outperforms traditional and lightweight dehazing networks in both PSNR and SSIM. Compared to dehazing methods with intricate networks, Figure 3 shows that DCDPN [4] and FFANet [5] have haze residual, indicating certain advantages for our CDCNet. Figure 4 shows that CDCNet achieves the best results on the real-world images. Table 2 shows that CDCNet surpasses all methods in CIEDE2000, demonstrating its superior color restoration.

### 3.3. Complexity and Runtime Analysis

Table 2 compares CDCNet with other SOTA methods based on network parameters, model size, and average execution time. With a model size of only 39.20 KB, CDCNet is compact but highly efficient, significantly smaller than most methods. For  $620 \times 460$  resolution images, the average execution time is 0.017 seconds, enabling real-time dehazing.

### 3.4. Ablation Study

Table 3 details the impact of each component on CDCNet's performance, indicating that each module distinctly enhances its comprehensive performance. Table 4 indicates that when

**Table 3.** Comparisons on SOTS for different variants of CD-CNet.

Variant	PSNR↑	SSIM↑
w/o Multi-scale Feature Aggregation Module	22.65	0.8489
w/o Attention Module	24.16	0.9211
<b>CDCNet</b>	<b>26.05</b>	<b>0.9518</b>

**Table 4.** Comparisons on HazeRD for different variants of CDCNet.

Variant	CIEDE2000↓
w/o proportional residual connection	11.713
w/o Lab and Contrast loss	11.694
w/o CDC Module	12.350
<b>CDCNet</b>	<b>11.559</b>

using the CDC module, even if one of the other methods is abandoned, the result still approximates the current best color restoration performance. This further illustrates the effectiveness of the CDC module.

## 4. CONCLUSION

In this paper, we propose a fast lightweight dehazing network with color distortion correction (CDCNet), which retains the dehazing performance and achieves real-time processing with lightweight. A post-processing module is introduced to compensate for the saturation and luminance in HSV and Lab color space. This approach rectifies the color distortions engendered by lightweight dehazing networks. Results show that our CDCNet surpasses state-of-the-art lightweight dehazing methods.

## Acknowledgements

This work was supported in part by the "Ling Yan" Program for Tackling Key Problems in Zhejiang Province (No.2022C01098), in part by the National Natural Science Foundation of China under Grant 62031009 and 62204044, in part by Alibaba Innovative Research (AIR) Program, in part by Alibaba Research Fellow (ARF) Program, in part by the Fudan-ZTE Joint Lab, in part by CCF-Alibaba Innovative Research Fund For Young Scholars.

## 5. REFERENCES

- [1] Weichen Xu and Tianhao Fu, “Overcoming the seesaw in monocular 3d object detection via language knowledge transferring,” in *ICASSP 2023 - 2023 IEEE International Conference on Acoustics, Speech and Signal Processing (ICASSP)*, 2023, pp. 1–5.
- [2] Alireza Jolfaei and Krishna Kant, “Privacy and security of connected vehicles in intelligent transportation system,” in *2019 49th Annual IEEE/IFIP International Conference on Dependable Systems and Networks—Supplemental Volume (DSN-S)*. IEEE, 2019, pp. 9–10.
- [3] Kaiming He, Jian Sun, and Xiaou Tang, “Single image haze removal using dark channel prior,” *IEEE transactions on pattern analysis and machine intelligence*, vol. 33, no. 12, pp. 2341–2353, 2010.
- [4] Qingsong Zhu, Jiaming Mai, and Ling Shao, “A fast single image haze removal algorithm using color attenuation prior,” *IEEE transactions on image processing*, vol. 24, no. 11, pp. 3522–3533, 2015.
- [5] He Zhang and Vishal M Patel, “Densely connected pyramid dehazing network,” in *Proceedings of the IEEE conference on computer vision and pattern recognition*, 2018, pp. 3194–3203.
- [6] Xu Qin, Zhilin Wang, Yuanchao Bai, Xiaodong Xie, and Huiyu Jia, “Ffa-net: Feature fusion attention network for single image dehazing,” in *Proceedings of the AAAI conference on artificial intelligence*, 2020, vol. 34, pp. 11908–11915.
- [7] Boyi Li, Xiulian Peng, Zhangyang Wang, Jizheng Xu, and Dan Feng, “An all-in-one network for dehazing and beyond,” *arXiv preprint arXiv:1707.06543*, 2017.
- [8] Dongdong Chen, Mingming He, Qingnan Fan, Jing Liao, Liheng Zhang, Dongdong Hou, Lu Yuan, and Gang Hua, “Gated context aggregation network for image dehazing and deraining,” in *2019 IEEE winter conference on applications of computer vision (WACV)*. IEEE, 2019, pp. 1375–1383.
- [9] Yong Liu and Xiaorong Hou, “Local multi-scale feature aggregation network for real-time image dehazing,” *Pattern Recognition*, vol. 141, pp. 109599, 2023.
- [10] Bolun Cai, Xiangmin Xu, Kui Jia, Chunmei Qing, and Dacheng Tao, “Dehazenet: An end-to-end system for single image haze removal,” *IEEE transactions on image processing*, vol. 25, no. 11, pp. 5187–5198, 2016.
- [11] Ketan Tang, Jianchao Yang, and Jue Wang, “Investigating haze-relevant features in a learning framework for image dehazing,” in *Proceedings of the IEEE conference on computer vision and pattern recognition*, 2014, pp. 2995–3000.
- [12] Jing Zhang and Dacheng Tao, “Famed-net: A fast and accurate multi-scale end-to-end dehazing network,” *IEEE Transactions on Image Processing*, vol. 29, pp. 72–84, 2019.
- [13] Kaiming He, Xiangyu Zhang, Shaoqing Ren, and Jian Sun, “Deep residual learning for image recognition,” in *Proceedings of the IEEE conference on computer vision and pattern recognition*, 2016, pp. 770–778.
- [14] Gao Huang, Zhuang Liu, Laurens Van Der Maaten, and Kilian Q Weinberger, “Densely connected convolutional networks,” in *Proceedings of the IEEE conference on computer vision and pattern recognition*, 2017, pp. 4700–4708.
- [15] Sanghyun Woo, Jongchan Park, Joon-Young Lee, and In So Kweon, “Cbam: Convolutional block attention module,” in *Proceedings of the European conference on computer vision (ECCV)*, 2018, pp. 3–19.
- [16] Dan Margulis, *Photoshop LAB color: The canyon conundrum and other adventures in the most powerful colorspace*, Peachpit Press, 2005.
- [17] Justin Johnson, Alexandre Alahi, and Li Fei-Fei, “Perceptual losses for real-time style transfer and super-resolution,” in *Computer Vision–ECCV 2016: 14th European Conference, Amsterdam, The Netherlands, October 11–14, 2016, Proceedings, Part II 14*. Springer, 2016, pp. 694–711.
- [18] Boyi Li, Wenqi Ren, Dengpan Fu, Dacheng Tao, Dan Feng, Wenjun Zeng, and Zhangyang Wang, “Benchmarking single-image dehazing and beyond,” *IEEE Transactions on Image Processing*, vol. 28, no. 1, pp. 492–505, 2018.
- [19] Yanfu Zhang, Li Ding, and Gaurav Sharma, “Hazerd: an outdoor scene dataset and benchmark for single image dehazing,” in *2017 IEEE international conference on image processing (ICIP)*. IEEE, 2017, pp. 3205–3209.
- [20] Wenqi Ren, Si Liu, Hua Zhang, Jinshan Pan, Xiaochun Cao, and Ming-Hsuan Yang, “Single image dehazing via multi-scale convolutional neural networks,” in *Computer Vision–ECCV 2016: 14th European Conference, Amsterdam, The Netherlands, October 11–14, 2016, Proceedings, Part II 14*. Springer, 2016, pp. 154–169.